Metal-Stabilized Methylene Arenium and σ-Arenium Compounds: Synthesis, Structure, Reactivity, Charge Distribution, and Interconversion

Arkadi Vigalok,† Boris Rybtchinski,† Linda J. W. Shimon,‡ Yehoshoa Ben-David,† and David Milstein*,†

Department of Organic Chemistry and Department of Chemical Services, The Weizmann Institute of Science, Rehovot 76100, Israel

Received November 30, 1998

Protonation of rhodium and iridium complexes of formula $ClM(CH_3)[C_6H(CH_3)_2(CH_2P(t\text{-}Bu)_2)_2]$ (M = Rh (**1**), Ir (**3**)) with a strong acid (HOTf, trifluoromethanesulfonic acid) results in clean formation of the new methylene arenium metal complexes $ClM[CH_2{=}C_6H(CH_3)_2(CH_2P(t\text{-}Bu)_2)_2]^+OTf^-$ (M = Rh (**2a**), Ir (**4**), respectively), which have been fully characterized including an X-ray single-crystal analysis. This new method can be applied to complexes having both electron-donating and electron-withdrawing substituents in the aromatic ring. The methylene arenium complexes bear most of the positive charge in the ring, resulting in their high CH acidity. Deprotonation of these complexes with NEt_3 gives the new metal xylylene complexes **12** (M = Rh) and **13** (M = Ir), which can be converted back to the methylene arenium complexes by reaction with HOTf. Reaction of the cationic complexes $^-OTf^+Rh(R)[C_6H(CH_3)_2(CH_2P(t\text{-}Bu)_2)_2]$ (R = CH_3, $PhCH_2$) with CO gives the new alkyl σ-arenium rhodium complexes $Rh(CO)[R{-}C_6H(CH_3)_2(CH_2P(t\text{-}Bu)_2)_2]^+OTf^-$ (R = CH_3 (**9a**), $PhCH_2$ (**9b**)). On the basis of the NMR data, the X-ray crystal structure analysis, and the reactivity, these Rh complexes were shown to have much less positive charge in the ring as compared to the methylene arenium complexes, most probably due to stabilization of an arene form by an agostic interaction of the arene−alkyl C_{ipso}−C bond with the metal center. The nature of the reported phenomena is discussed. The interconversion of the methylene arenium and alkyl σ-arenium metal complexes is also presented.

Introduction

Coordination of a metal ion to the π-system of an aromatic ring results in substantial perturbations of the aromaticity in the organic compound.[1] This type of interaction has been extensively explored for the last few decades, and it is successfully applied in both organic and organometallic synthetic transformations.[2,3] Recently, Harman and co-workers have shown that even η^2-type coordination of a transition metal cation to aromatics dramatically changes the reactivity of the latter toward electrophiles and sometimes promotes irreversible loss of aromaticity.[4] However, a class of metal complexes with a more perturbed (partially destroyed) aromatic system, arenium complexes, is practically unexplored. Although Wheland-type σ-arenium metal complexes are thought to be crucial intermediates in electrophilic metalation of aromatics,[5] the NCN pincer Pt(II) complexes reported by van Koten and co-workers have remained for a long period the only examples of isolated metal σ-arenium species.[6] We have recently reported unique stable *methylene arenium* compounds stabilized by complexation via an exocyclic double bond to a late transition metal center in the bischelated PCP-type system.[7] As these complexes were initially obtained by protonation of the rare quinone methide[8] or xylylene[7] metal complexes their generation was limited to methylene cyclohexadiene metal precursors.

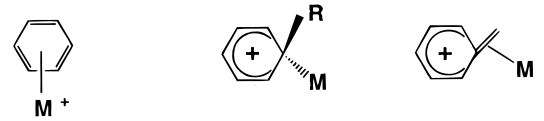

π-arene complex σ-arenium methylene arenium

We now present a new general approach to PCP-type methylene arenium complexes, starting from metal aryl

* Corresponding author. E-mail: comilst@wiccmail.weizmann.ac.il.
† Department of Organic Chemistry.
‡ Department of Chemical Services.

(1) (a) Collman, J. P.; Hegedus, L. S.; Norton, J. R.; Finke, R. G. In *Principles and Applications of Organotransition Metal Chemistry*; University Science Books: Mill Valley, California, 1987. (b) Vogel, P. *Carbocation Chemistry*; Elsevier: New York, 1985.

(2) (a) Astruc, D. *Tetrahedron* **1983**, *39*, 4027. (b) Pike, R. D.; Sweigart, D. A. *Synlett* **1990**, 565. (c) Semmelhack, M. F. In *Comprehensive Organic Chemistry*; Trost, B. M., Fleming, I., Eds.; Pergamon Press: Oxford, 1991; Vol. 4, 517.

(3) Hegedus, L. S. *Transition Metals in the Synthesis of Complex Organic Molecules*; University Science Books: Mill Valley, CA, 1994; Chapter 10, p 307.

(4) (a) Winemiller, M. D.; Kopach, M. E.; Harman, W. D. *J. Am. Chem. Soc.* **1997**, *119*, 2096. (b) Harman, W. D. *Chem. Rev.* **1997**, *97*, 1953, and references therein.

(5) Taylor, R. *Electrophilic Aromatic Substitution*; John Wiley & Sons: New York, 1990.

(6) (a) Grove, D. M.; van Koten, G.; Louwen, J. N.; Noltes, J. G.; Spek, A. L.; Ubbels, H. J. C. *J. Am. Chem. Soc.* **1982**, *104*, 6609. (b) Terheijden, J.; van Koten, G.; Vinke, I. C.; Spek, A. L. *J. Am. Chem. Soc.* **1985**, *107*, 2891.

(7) Vigalok, A.; Shimon, L. J. W.; Milstein, D. *J. Am. Chem. Soc.* **1998**, *120*, 477.

(8) Vigalok, A.; Milstein, D. *J. Am. Chem. Soc.* **1997**, *119*, 7873.

10.1021/om980960i CCC: $18.00
Publication on Web 02/04/1999

precursors, which involves loss of aromaticity under very mild conditions. A new approach to σ-arenium metal complexes is also presented, and the structure and reactivity of these rare species, stabilized by an unusual agostic interaction of a C−C bond with a metal center, are described.

Results

Synthesis of Methylene Arenium Rhodium Complexes. When the methyl chloride Rh(III) complex **1a**[9] was reacted with one or more equivalents of triflouromethanesulfonic (triflic) acid in CH_2Cl_2, a color change from red to green took place and the new methylene arenium complex **2a** was quantitatively formed (eq 1).

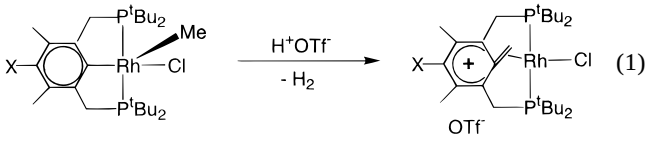

(1)

1 **2**

1,2: X=H (a), OH (b), CO_2Me (c)

Complex **2a** was unequivocally characterized by multinuclear NMR spectroscopy and by X-ray structure analysis. The $^{31}P\{^1H\}$ NMR spectrum of **2a** consists of a doublet at 17.55 ppm (J_{RhP} = 98.0 Hz). The ^1H NMR spectrum shows a broad triplet at 4.84 ppm (J_{PH} = 6.5 Hz) due to the coordinated methylene group. The ring-bound hydrogen atom exhibits a single resonance at 8.60 ppm, a characteristic downfield shift for positively charged arenium species.[10] In the $^{13}C\{^1H\}$ NMR spectrum the coordinated double bond gives rise to a pair of doublets of triplets centered at 93.37 ppm (J_{RhC} = 8.3 Hz, J_{PC} = 3.1 Hz, Rh(**C**=CH_2)) and at 41.47 ppm (J_{RhC} = 24.7 Hz, J_{PC} = 2.7 Hz, Rh(C=**C**H_2)). In the same spectrum the ortho- and para-carbon atoms show two singlets at 160.80 ppm and at 151.23 ppm, respectively, indicating a relatively high degree of the positive charge localization at these carbons.[10]

Green needles of **2a** suitable for a single-crystal X-ray analysis have been obtained by slow crystallization from a CH_2Cl_2/THF (1:1) solution. The structure of **2a** (Figure 1) shows that the Rh atom is situated in the center of a square plane with the coordinated double bond being tilted toward the chlorine atom. Selected bond lengths and bond angles are presented in Table 1. The positively charged arenium ring exhibits unsymmetrical charge distribution similar to what was observed for its phenolic analogue **2b**[7] (vide infra); however there is considerable averaging of the bond distances of the ring as a result of more effective positive charge delocalization due to lack of the stabilizing OH group. For example, the bond lengths C(12)−C(13) and C(15)−C(16) (1.390(7) and 1.398(8) Å, respectively) in **2a** are longer than those in **2b** (1.373(6) and 1.382(6) Å, respectively), whereas the bond lengths C(13)−C(14) (1.404(7) Å) and C(14)−C(15) (1.408(8) Å) are shorter than that in **2b** (1.416(6) and 1.415(6) Å, respectively). The coordinated

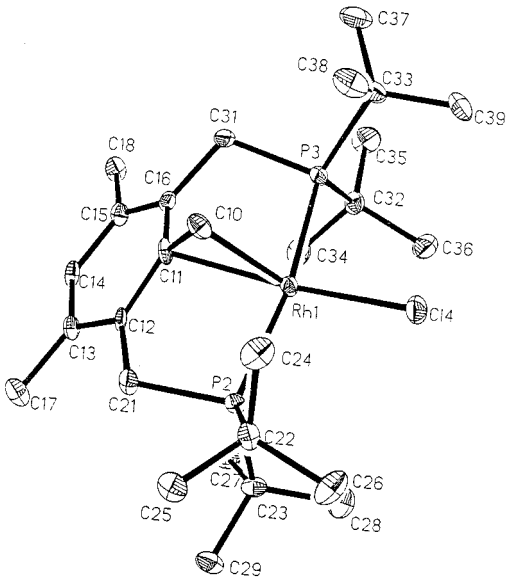

Figure 1. ORTEP view of a cation of **2a** with the thermal ellipsoids at 50% probability. The hydrogen atoms are omitted for clarity.

Table 1. Selected Bond Lengths (Å) and Angles (deg) for 2a

(a) Bond Lengths

Rh(1)−C(10)	2.022(6)	C(11)−C(12)	1.427(7)
Rh(1)−C(11)	2.259(5)	C(12)−C(13)	1.390(7)
C(10)−C(11)	1.445(7)	C(13)−C(14)	1.404(7)
Rh(1)−Cl(4)	2.310(2)	C(14)−C(15)	1.408(8)
Rh(1)−P(2)	2.352(2)	C(15)−C(16)	1.398(8)
Rh(1)−P(3)	2.355(2)	C(11)−C(16)	1.452(7)

(b) Angles

P(2)−Rh(1)−P(3)	168.68(5)	C(10)−C(11)−Rh(1)	61.6(3)
P(2)−Rh(1)−C(10)	87.7(2)	C(12)−C(11)−C(16)	120.9(5)
P(2)−Rh(1)−C(11)	85.1(2)	C(13)−C(14)−C(15)	124.6(5)
C(10)−Rh(1)−C(11)	39.0(2)	C(11)−C(12)−C(13)	119.1(5)
Rh(1)−C(10)−C(11)	79.4(3)	C(12)−C(13)−C(14)	118.2(5)

C(10)−C(11) double-bond length of 1.445(7) Å compares well to that in **2b** (1.452(6) Å),[7,8,11] as well as the Rh(1)−C(10) bond length of 2.022(6) Å vs 2.032(5) in **2b**. However, there is a small but noticeable lengthening of the Rh(1)−C(11) bond (2.259(5) Å in **2a** vs 2.229(4) Å in **2b**), possibly due to a weaker interaction of the metal center with the positively charged ring.

When the methyl chloride rhodium(III) complex **1b** was treated with triflic acid, the known methylene arenium compound **2b**[7] was formed quantitatively, showing that this approach can be applied with methyl rhodium compounds regardless of the substituent in the para-position. To verify this, the new methyl chloride rhodium(III) complex **1c**, having an electron-withdrawing CO_2Me group in the para-position, was synthesized (Scheme 1).

When **1c** was reacted with triflic acid, the methylene arenium complex **2c** was quantitatively produced (eq 1), showing that *no stabilizing substituents in the ring are required* for the generation of methylene arenium complexes, i.e., that the method is general with respect to the aromatic moiety and can be applied to a variety

(9) Rybtchinski, B.; Vigalok, A.; Ben-David, Y.; Milstein, D. *J. Am. Chem. Soc.* **1996**, *118*, 12406.

(10) Koptyug, V. A. *Contemporary Problems in Carbonium Ion Chemistry III*, in Topics in Current Chemistry 122; Springer-Verlag: Berlin, 1984.

(11) For other examples of rhodium-coordinated double-bond lengths in bischelating systems see: (a) Vigalok, A.; Shimon, L. J. W.; Milstein, D. *J. Chem. Soc., Chem. Commun.* **1996**, 1673. (b) Vigalok, A.; Kraatz, H.-B.; Konstantinovsky, L.; Milstein, D. *Chem. Eur. J.* **1997**, *3*, 253. (c) Mason, R.; Scollary, G. R. *Aust. J. Chem.* **1978**, *31*, 781.

Scheme 1

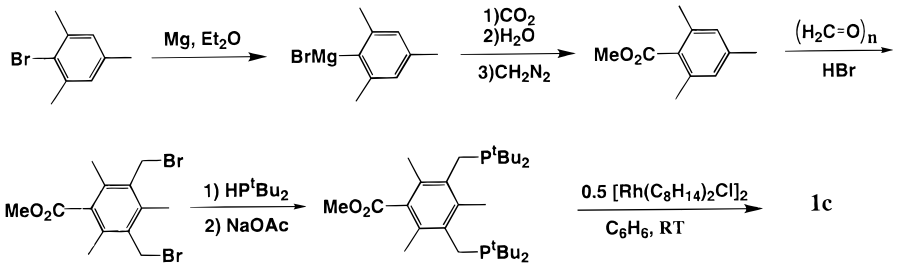

of PCP-type complexes. The NMR spectra of complex **2c** are very similar to those of **2a** (see Experimental Section). The $^{13}C\{^1H\}$ NMR spectrum of **2c** indicates no significant effect of the para-substituent on the chemical shift of the coordinated methylene group, complex **2c** showing a doublet of triplets at 39.59 ppm (J_{RhC} = 24.6 Hz, J_{PC} = 3.1 Hz) vs 41.47 ppm in **2a**.

Synthesis of a Methylene Arenium Iridium Complex. The approach described here for the generation of arenium complexes is not limited to rhodium. Upon reaction of the iridium(III) complex **3**[9] with a slight excess of HOTf, complete conversion into the new methylene arenium complex **4** was achieved (eq 2). Complex **4** exhibits a dramatic upfield shift in the $^{31}P\{^1H\}$ NMR spectrum (s, 12.70 ppm) in comparison to the starting **3** (s, 45.37 ppm). In the ^1H NMR spectrum the aromatic proton appears as a singlet at 9.20 ppm, which is a very low field region even for positively charged arenium species.[10] The coordinated olefin gives rise to a triplet in the ^1H NMR spectrum at 5.18 ppm (J_{PC} = 6.6 Hz). In the $^{13}C\{^1H\}$ NMR spectrum of **4** there is a broad singlet at 35.48 ppm due to the coordinated methylene carbon and a broad singlet at 83.14 ppm due to the quaternary carbon. The downfield shift of the aromatic carbon atoms in the $^{13}C\{^1H\}$ NMR spectrum (169.28 ppm, ortho; 152.59 ppm, para) is consistent with the formation of the charged arenium species.[10] It is important that the ^1H NMR and the $^{13}C\{^1H\}$ NMR spectra of the iridium complex **4** indicate more positive charge on the ring as compared with the rhodium analogue **2a**.

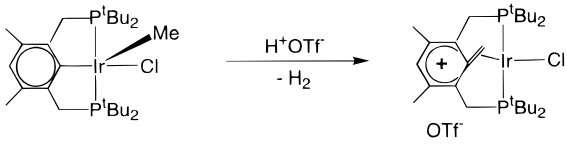

3 4 (2)

Low-Temperature NMR Study of Protonation of Complexes 1a and 3. When **1a** was treated with 5 equiv of triflic acid in $CDCl_3$ at −55 °C, formation of a single product **5** immediately took place. The same compound was observed upon protonation of **1a** in CD_2Cl_2 at −85 °C (Scheme 2). The $^{31}P\{^1H\}$ NMR spectrum of **5** at −55 °C consists of a doublet at 52.52 ppm (J_{RhP} = 92.7 Hz). The ^1H NMR spectrum shows a doublet of triplets centered at −21.38 ppm (J_{RhH} = 34.2 Hz) for the hydride ligand and a broad singlet at 3.47 ppm due to the coordinated methylene group. The same group gives rise to a broad doublet in the $^{13}C\{^1H\}$ NMR spectrum at 48.25 ppm (J_{RhC} = 7.4 Hz). Upon warming above −40 °C complex **5** slowly underwent deprotonation to give **2a** (Scheme 2). The rate of HOTf loss was dependent on the concentration of HOTf present in the system. No protonation of **2a** to give **5** was observed when the former was exposed to a large excess of HOTf in dichloromethane, showing that **2a** is the thermodynamically most stable product in the system. Surprisingly, when **1a** was reacted with 5 equiv of *D*OTf in $CDCl_3$ at −55 °C, only formation of **5** was observed with *no deuterium incorporation* either into the methylene group or into the hydride. In the reaction of **1a** with 1 equiv of HOTf at low temperature, complex **5** was observed in a mixture of several other products. Upon warming up all of the intermediates converted into complex **2a**.

Scheme 2. Postulated Mechanism of Formation of the Methylene Arenium Complexes[a]

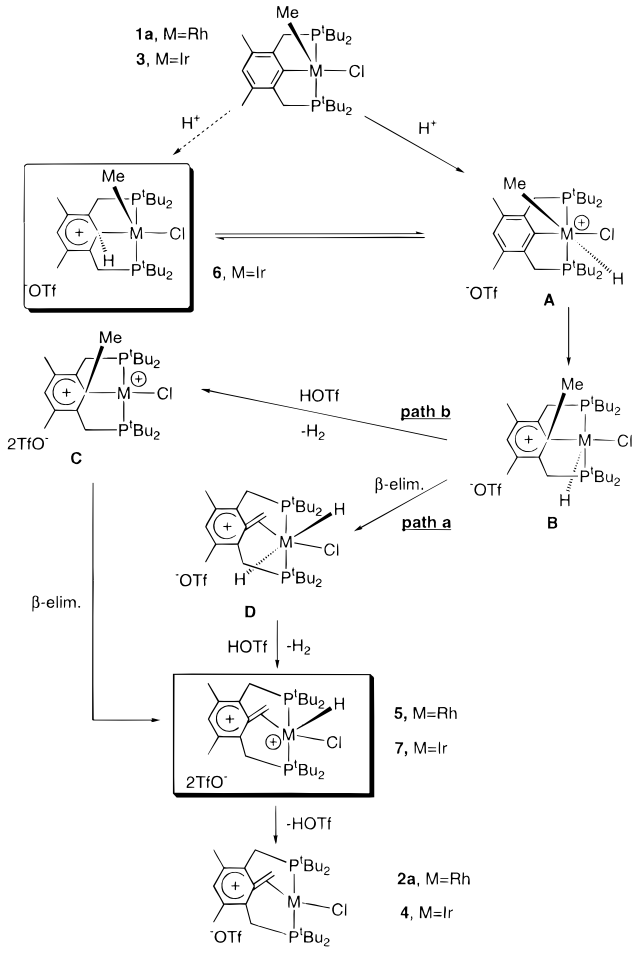

[a] The spectroscopically characterized compounds are numbered and given in frames; postulated intermediates are assigned with capital letters.

When a large excess (9 equiv in $CDCl_3$) of triflic acid was added to a $CDCl_3$ solution of the iridium complex **3** at −55 °C, the $^{31}P\{^1H\}$ NMR spectrum of the mixture after 15 min showed four main singlets: at 49.03 ppm, 44.61 ppm (starting complex **3**), 43.38 ppm, and 39.21 ppm, in a ratio of 10:4:5:15, respectively. After ca. 15 min at −40 °C $^{31}P\{^1H\}$ NMR revealed formation of two main products as singlets at 49.11 and 39.47 ppm, in a ratio of 1:2, respectively. The first product, assigned as complex **6**, exhibits in ^1H NMR characteristic signals at 3.44 ppm (broad singlet, 1H, **H**−ipso-C, no signal when DOTf was used) and at 1.84 ppm (t, J_{PH} = 4.9 Hz, 3H, Ir−C**H**$_3$), and in the $^{13}C\{^1H\}$ NMR spectrum a triplet at −26.66 ppm (J_{PC} = 4.3 Hz, Ir−**C**H$_3$). Characteristic signals attributed to the second product, complex **7**, in ^1H NMR (ppm) are 3.73 (unresolved triplet, 2H, =C**H**$_2$), −35.78 (t, J_{PH} = 8.7 Hz, **H**−Ir). The signal assignment was based on integration and on the observation of **7** as the main product at 0 °C (vide infra). This assignment was confirmed by $^1H\{^{31}P\}$ NMR.

As the temperature was gradually raised to 0 °C, complex **7** became the main product in the reaction mixture (∼70%, observed by $^{31}P\{^1H\}$ NMR). The ^1H NMR signal of the coordinated methylene was resolved into a triplet at this temperature (3.75 ppm, J_{PH} = 3.4 Hz). The hydride signal integration was not changed when DOTf was used. Only a small amount of the final product, complex **4**, was observed at this stage. As the temperature was raised to 20 °C, slow formation of the final product **4** took place. Staying at room temperature overnight resulted in formation of **4** (ca. 90%) and decomposition products.

When 1−1.5 equiv of HOTf was added to a $CDCl_3$ solution of **3** at −55 °C, $^{31}P\{^1H\}$ NMR and ^1H NMR spectra revealed simultaneous formation of **6** and **7** together with other products. Gradual heating to 0 °C resulted in clean formation of **4**. The reaction was complete after about 1 h at this temperature.

The mechanism of the proton-induced rearrangement of the metal(III) methyl chloride complexes appears to be complicated, with several equilibria taking place simultaneously. It is conceivable that the initial proton attack at the metal gives the trans hydrido-methyl M(V) complex **A** (Scheme 2). This electron-poor species must be very unstable, and a 1,2-methyl shift to give the methyl arenium complex **B** may take place. Such an apparent 1,2-methyl shift upon reducing electron density on the metal was observed in the synthesis of the σ-arenium complexes reported here (vide infra), so the formation of a σ-arenium intermediate **B** seems a likely process. A 1,2-hydride shift in **A** or an initial attack of the proton on the ipso-carbon is also possible, forming complex **6** in the case of iridium. These reaction pathways, however, are degenerate, as is the reversible HOTf dissociation from this complex. Complex **B** can then undergo β-hydrogen elimination giving the trans dihydride **D**, which can react with free HOTf to give the observed deprotonated hydrido-triflates **5** and **7** (path a). However, the deprotonation of the trans-dihydride **D** is not expected to be very selective. As *no deuterium labeling* in complexes **5** and **7** for Rh and Ir, respectively, was observed when *D*OTf was used, a pathway with deprotonation *prior* to β-hydrogen elimination to form a dicationic species **C** (path b) is more likely. Formed from **C** by β-H elimination, complexes **5** and **7** undergo spontaneous loss of triflic acid at temperatures above −40 °C (Rh) or 0 °C (Ir). To the best of our knowledge, HOTf loss from trivalent Rh and Ir phosphine complexes under such mild conditions is unprecedented. The t-Bu−PCP benzylic hydrido chloride Ir(III) complex[9] does *not* give complex **4** upon reaction with HOTf. So, it is conceivable that metal bonding to the aromatic ring is critical for the whole process and that a 1,2 shift without metal detachment from the ring indeed takes place on the reaction pathway.

Synthesis of σ-Arenium Complexes. When the cationic Rh(III) complex **8a** was reacted with CO in THF or in $CDCl_3$ at room temperature, immediate formation of the methyl arenium Rh(I) complex **9a** took place as a result of an *apparent 1,2-methyl shift* (eq 3). Low-temperature experiments showed no traces of possible intermediates in this reaction, which proceeds smoothly even at −60 °C. The $^{31}P\{^1H\}$ NMR spectrum of **9a** consists of a doublet at 25.14 ppm (J_{RhP} = 99.1 Hz). The methyl group bound to the ipso-carbon gives rise to a broad singlet in the ^1H NMR spectrum at 2.59 ppm, whereas the proton bound to the ring gives a singlet at 7.19 ppm. The ipso-carbon appears as a triplet of doublets at 108.53 ppm in the $^{13}C\{^1H\}$ NMR spectrum, with the coupling constant J_{RhC} = 2.3 Hz being small for a regular $^1J_{RhC}$. In other PCP-type Rh complexes the latter is normally as large as 30 Hz.[9,12] In the same spectrum the methyl group at the ipso-carbon appears far upfield at 8.23 ppm as a broad multiplet due to couplings to Rh and two phosphorus nucleii.

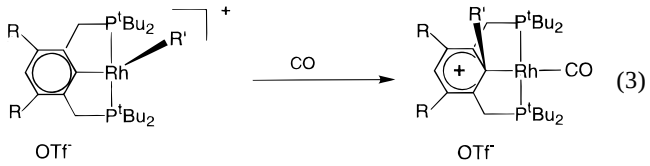

(3)

R= R'= Me: **8a** R= R'= Me: **9a**

R= Me, R'= CH_2Ph: **8b** R= Me, R'= CH_2Ph: **9b**

R= R'= H: **10** R= R'= H: **11**

Similarly, reaction of the benzyl triflate Rh(III) complex **8b** with carbon monoxide resulted in a *1,2-benzyl shift* and formation of the benzyl arenium complex **9b** (eq 3). Complex **9b** was characterized by multinuclear NMR spectroscopy, and its NMR features are similar to those of **9a**, except that the CH_2Ph group bound to the ipso-carbon appears in the ^1H NMR spectrum at 4.95 ppm as a singlet.

Orange plates of complex **9b** suitable for a single-crystal X-ray analysis were obtained by slow evaporation of a THF solution. A molecular view of a cation of **9b** is shown in Figure 2. The X-ray structure of **9b** confirms the apparent 1,2-benzyl shift taking place, with the benzyl group being directly attached to the ipso-carbon atom. Although the connectivity in **9b** is unequivocally determined by the X-ray structure analysis, the relatively poor quality of the crystal does not allow detailed discussion of the most interesting crystallographic features. However, we were able to crystallize

(12) Vigalok, A.; Ben-David, Y.; Milstein, D. *Organometallics* **1996**, *15*, 1838.

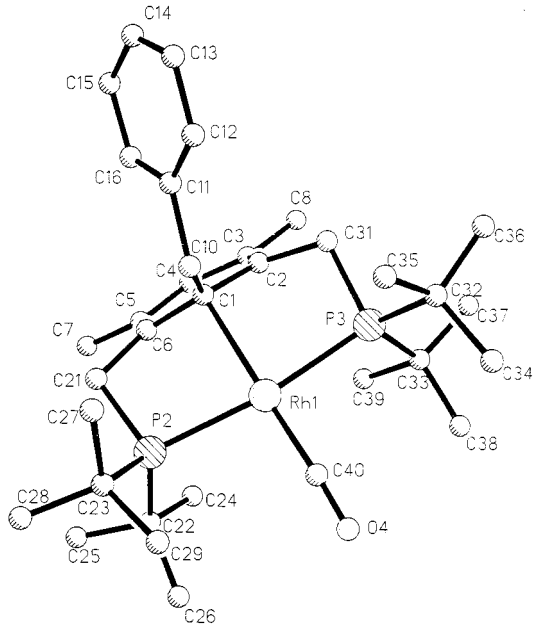

Figure 2. Molecular view of a cation of **9b**. The hydrogen atoms are omitted for clarity.

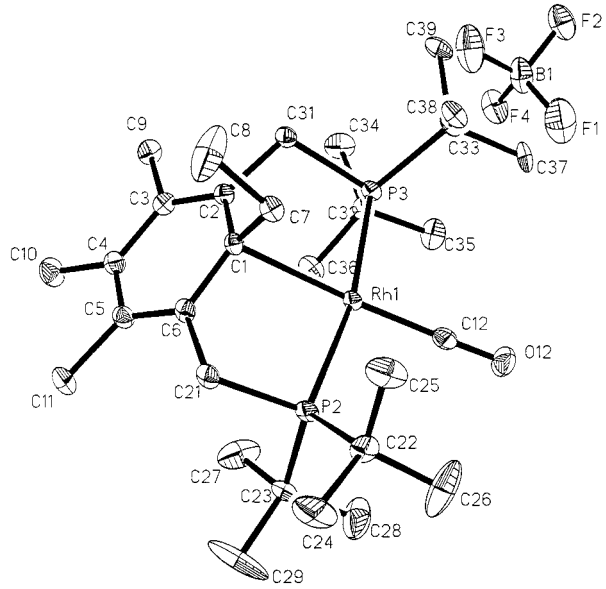

Figure 3. ORTEP view of a molecule of **9c** with the thermal ellipsoids at 50% probability. The hydrogen atoms are omitted for clarity.

the close analogue of **9b**, the ethyl arenium complex **9c**,[13] which was subjected to a single-crystal X-ray analysis. An ORTEP representation of a molecule of **9c** is shown in Figure 3. Selected bond lengths and bond angles are given in Table 2. There is only small bond alternation in the aromatic ring. The C(2)−C(3) and C(5)−C(6) bond distances of 1.395(4) and 1.399(4) Å, respectively, are only slightly shorter than the rest of the ring. The ipso-carbon atom is removed out of the plane (ca. 0.108 Å). The distance between this carbon and the rhodium atom of 2.354(4) Å is, however, very long for a regular Rh−C bond (compare, for example, to 2.259(5) Å in the olefinic **2a**). Interestingly, the distance between the rhodium atom and C(7) of 2.817 Å is shorter than the sum of the van der Waals radii of the two atoms, assuming some sort of interactions between the two (vide infra). The Rh(1)−C(1)−C(7) bond angle of 90.25(16)° is substantially smaller than that in a tetrahedron, which speaks against the extreme arenium representation of **9c**.

(13) Milstein, D. To be submitted.

Table 2. Selected Bond Lengths (Å) and Angles (deg) for 9c

(a) Bond Lengths			
Rh(1)−C(12	1.811(3)	C(2)−C(3)	1.395(4)
Rh(1)−C(1)	2.354(3)	C(3)−C(4)	1.414(4)
C(1)−C(7)	1.537(4)	C(4)−C(5)	1.410(4)
Rh(1)−P(2	2.3404(8)	C(5)−C(6)	1.399(4)
C(7)−C(8)	1.521(4)	C(1)−C(6)	1.434(4)
C(1)−C(2)	1.435(3)	Rh(1)···C(10)	2.817
(b) Angles			
P(2)−Rh(1)−P(3)	169.21(3)	C(2)−C(3)−C(4)	119.0(2)
P(2)−Rh(1)−C(1)	84.62(7)	C(3)−C(4)−C(5)	121.6(3)
Rh(1)−C(1)−C(7)	90.25(16)	C(1)−C(2)−C(3)	120.4(2)
C(2)−C(1)−C(6)	119.0(2)	C(4)−C(5)−C(6)	119.7(3)
C(8)−C(7)−C(1)	108.7(2)	C(1)−C(2)−C(31)	117.0(2)

Reactivity of the Methylene Arenium and σ-Arenium PCP Complexes. Due to the positive charge in the ring, both the Rh (**2a**) and Ir (**4**) methylene arenium complexes are strong CH acids and can be deprotonated by relatively weak organic bases to give the corresponding ortho-xylylene metal complexes, **12** and **13**, respectively (eq 4).

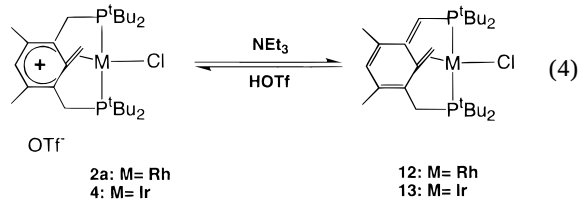

(4)

In both cases the metal is coordinated to only one of the exocyclic double bonds.[15] The rhodium xylylene complex **12** shows NMR data similar to the previously reported Rh−Me xylylene complex.[7] For example, it exhibits an AB pattern in the $^{31}P\{^1H\}$ NMR spectrum at 51.18 ppm (J_{PaPb} = 376.3 Hz, J_{RhPa} = 124.7 Hz, J_{RhPb} = 118.0 Hz), and the vinylic proton gives rise to a doublet at 5.28 ppm (J_{PH} = 3.4 Hz). The iridium methylene arenium complex **4** can be deprotonated with NEt_3 or alumina forming a red ortho-xylylene complex **13**. It gives rise to an AB quartet in $^{31}P\{^1H\}$ NMR centered at 36.94 ppm (J_{PP} = 360.1 Hz) as expected for two nonequivalent trans-P atoms. Other signals are also consistent with an unsymmetrical xylylene structure and are similar to those reported for a rhodium ortho-xylylene complex.[7] The assignment of ^1H and $^{13}C\{^1H\}$

(14) Vigalok, A.; Uzan, O.; Shimon, L. J. W.; Ben-David, Y.; Martin, J. M. L.; Milstein D. *J. Am. Chem. Soc.* **1998**, *120*, 12539.

(15) For recent review on metal centers coordinated to more than one double bond of a xylylene ligand see: Bennett, M. A. *Coord. Chem. Rev.* **1997**, *166*, 225.

NMR signals was confirmed by a 2D $^{13}C-^{1}H$ correlation. To the best of our knowledge complex **13** is the first reported iridium xylylene complex. The deprotonation of complexes **2a** and **4** is reversible. Upon addition of HOTf to $CDCl_3$ solutions of the rhodium or iridium xylylene complexes **12** or **13**, respectively, a color change from red to green-brown was observed in both cases. $^{31}P\{^{1}H\}$ and ^{1}H NMR revealed quantitative formation of the methylene arenium complexes **2a** and **4**, respectively.

Upon bubbling of carbon monoxide through a solution of **2a** in CD_2Cl_2, immediate color change from green to red took place and quantitative formation of the pentacoordinate CO adduct **14** was observed (eq 5). Complex **14** shows a doublet in the $^{31}P\{^{1}H\}$ NMR spectrum at 38.46 ppm ($J_{RhP} = 75.7$ Hz). The coordinated double bond gives rise to a triplet in the ^{1}H NMR spectrum at 4.15 ppm and to two signals in the $^{13}C\{^{1}H\}$ NMR spectrum at 107.69 ppm (**C**=CH_2) and at 39.10 ppm (C=**C**H_2). Complex **14** appears to be stable only under a CO atmosphere in solution. Moderate heating of a solution of **14** in methylene chloride or drying of **14** in a vacuum resulted in carbon monoxide loss and formation of **2a**. However, upon addition of Me_3SiOTf to a methylene chloride solution of **14**, slow Cl^- abstraction took place[16] to give the tetracoordinated dicationic complex **15** (eq 5). Complex **15** is more stable than **14** toward loss of CO and could be isolated as an orange solid. The $^{31}P\{^{1}H\}$ NMR spectrum of **15** exhibits a doublet at 35.65 ppm ($J_{RhP} = 76.3$ Hz). The coordinated methylene group gives rise to a triplet in the ^{1}H NMR spectrum at 4.47 ppm, whereas the arenium ring proton appears as a singlet at 7.98 ppm. The $^{13}C\{^{1}H\}$ NMR spectrum of **15** shows two signals for the coordinated double bond at 105.61 ppm and at 42.32 ppm for the quaternary carbon and the methylene carbon, respectively. The IR spectrum shows a strong CO absorption band at 2063 cm^{-1}, reflecting very little back-bonding to the carbonyl ligand, similar to what was observed for a related dicationic methylene arenium rhodium(I) complex.[7]

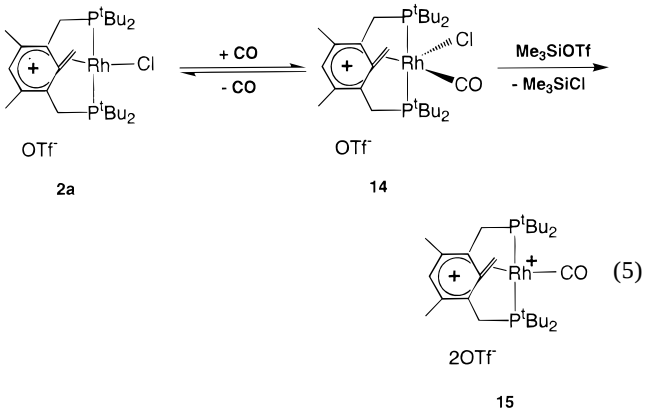

(5)

Interestingly, when dihydrogen was passed for several seconds through a solution of the dicationic complex **15** in CH_2Cl_2, clean formation of the methyl σ-arenium complex **9a** took place (eq 6). Complex **2a** failed to react with H_2 under the same conditions, whereas complex **4**

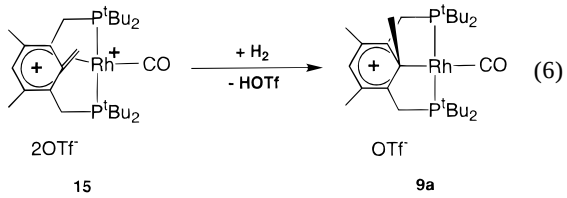

(6)

gives a complex mixture of products. Reactions of **9a** with nucleophiles, such as amines or MeO^-, did not result in ring adducts, as in the case of analogous van Koten's NCN Pt σ-arenium complex. Instead, deprotonation of the methyl group at the ipso-carbon atom took place with formation of the neutral benzylic Rh(I) complex **16** (eq 7). The latter complex shows a doublet in the $^{31}P\{^{1}H\}$ NMR spectrum at 109.73 ppm ($J_{RhP} = 170.5$ Hz). It also gives rise to a triplet of doublets in the ^{1}H NMR spectrum at 2.34 ppm ($J_{RhH} = 2.2$ Hz) due to the metal-bound benzylic group. The same group appears in the $^{13}C\{^{1}H\}$ NMR spectrum at 22.13 ppm as a doublet of triplets ($J_{RhC} = 12.4$ Hz). The deprotonation of **9a** giving **16** is a reversible process; reaction of **16** with HOTf gives **9a** quantitatively.

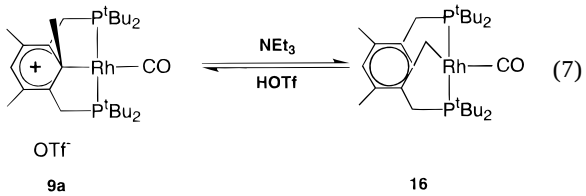

(7)

Discussion

Methylene Arenium Complexes. Utilization of readily available PCP metal aryl complexes for the synthesis of methylene arenium compounds provides a straightforward route to these rare species. The most remarkable feature of the process is the loss of aromaticity under very mild conditions. Dearomatization to form arenium cations, common intermediates in electrophilic aromatic substitution, is a process of primary importance in organic and organometallic chemistry.[1,5] Arenium ions have been generated by a variety of methods in the absence of a transition metal, requiring special design of reagents and substrates in order to stabilize the arenium species.[10,17,18] As for metal promoted dearomatization, protonation of $[Os(NH_3)_5(\eta^2\text{-arene})](OTf)_2$ to give η^2- or η^3-arenium complexes was reported.[4] In our cases, a σ-aryl rather than an arene complex is protonated, forming an arenium complex in which the π-system of the ring *is not involved* in coordination to the metal. The generality of the dearomatization process was demonstrated for different types of para-substituted aryl complexes, bearing both

(16) For a method for halide abstraction from a metal center using Me_3SiOTf see: Aizenberg, M.; Milstein, D. *J. Chem. Soc., Chem. Commun.* **1994**, 411.

(17) (a) Brouwer, D. M.; Mackor, E. L.; MacLean, C. In *Carbonium Ions*; Olah, G. A., von R. Schleyer, P., Eds.; 1970; Vol. 2, p 837. (b) Farcasiu, D. *Acc. Chem. Res.* **1982**, *15*, 46. (c) Farcasiu, D.; Marino, G.; Miller, G.; Kastrup, R. V. *J. Am. Chem. Soc.* **1989**, *111*, 7210. (d) Effenberger, F. *Acc. Chem. Res.* **1989**, *22*, 27. (e) Xu, T.; Barich, D. H.; Torres, P. D.; Haw, J. F. *J. Am. Chem. Soc.* **1997**, *119*, 406, and references therein.

(18) For crystallographically characterized organic σ-arenium complexes see: (a) Effenberger, F.; Reisinger, F.; Schönwälder, K. H.; Bäuerle, P.; Stezowski, J. J.; Jogun, K. H.; Schöllkopf, K.; Stohrer, W.-D. *J. Am. Chem. Soc.* **1987**, *109*, 882, and references therein. (b) Baenziger, N. C.; Nelson, A. D. *J. Am. Chem. Soc.* **1968**, *90*, 6606. (c) Borodkin, G. I.; Nagi, Sh. M.; Bagryanskaya, I. Yu.; Gatilov, Yu. V. *J. Struct. Chem.* (Russian) **1984**, *25*, 440.

e-donating and e-withdrawing substituents, and for two metals. A transition metal center plays a major role in the overall dearomatization, promoting proton-to-hydride transformaton, 1,2-methyl shift, and β-H elimination, a sequence of processes that leads to loss of aromaticity and formation of methylene arenium compounds. This complicated sequence of reactions leads to a seemingly simple outcome: net deprotonation of the methyl aryl complexes. However, stabilizing otherwise very unstable arenium intermediates and the final product is a unique consequence of the metal-controlled reactivity. Importantly, the presented results demonstrate that the ability of the metal to eliminate H_2 and to form a strong bond with the olefin moiety can overcome strong thermodynamic aromatization driving forces. The rigid chelating PCP system seems to be an important stabilizing factor too.

Alkyl σ-Arenium Metal Complexes. Although Wheland-type arenium species are thought to be crucial intermediates in electrophilic metalation of aromatics,[1,5] the NCN pincer Pt(II) complexes reported by van Koten and co-workers have remained for a long period the sole examples of isolated metal arenium species.[6,19] They were synthesized by adding methyl iodide (or triflate) to the NCN Pt(II) complexes and exhibit arenium reactivity: various nucleophiles attack the positively charged ring, resulting in adducts.[20]

In the system reported here, we observe direct apparent 1,2-alkyl shift upon CO addition to a rhodium aryl cationic complex.[21] Only "partial" dearomatization takes place here.

The crystal structure of **9c** reveals slight distortion in the aryl ring, assignable to arenium formation. However, the alkyl arenium complexes **9** still do not exhibit chemical properties expected for normal arenium species. For example, reaction of **9a** with nucleophiles does not give ring adducts as observed in cases of the platinum arenium complexes,[20] although deprotonation of the methyl group at the ipso-carbon does take place, forming the benzyl Rh(I) complex **16** (eq 7). This, together with ^{1}H and ^{13}C NMR of **9**, which show less downfield shifts than expected for an arenium species, suggests that the positive charge on the ring is somewhat reduced. We explain it by the fact that in the σ-alkyl arenium complex there is a partial negative charge on the ipso-carbon and some electron density can be donated to the π-system, leading to partial aromatization. Thus, complex **9** can be viewed as a mixture of arenium and arene resonance forms (Scheme 3). In the case of van Koten's NCN Pt-arenium complexes[6] some contribution of the arene form is probably also present; however it seems to be significantly less than in the case of **9**, based on a comparison of ^{1}H and ^{13}C NMR signals and reactivity of these two groups of compounds.[6] Thus, interestingly, a Pt(II) complex with amine ligands appears to be better than a Rh(I) phosphine complex for stabilizing the arenium resonance form.

An agostic interaction of the C−C bond with the metal, stabilizing the arene resonance form, probably

Scheme 3

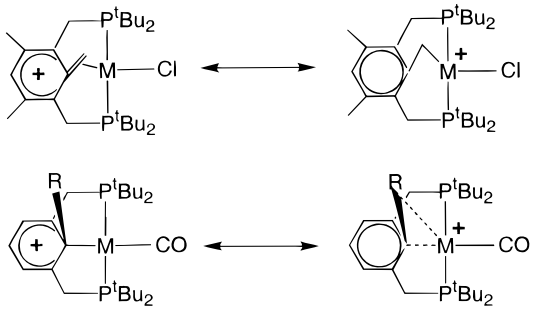

also contributes to the overall energy of complex **9**. The alkyl groups at C_{ipso} NMR signals of **9** show coupling due to the ^{103}Rh nucleus, and the crystal structure of **9c** reveals that the metal−ethyl C distance of 2.817 Å is within the sum of the van der Waals radii of the two atoms. The Rh−ipso-C bond distance of 2.354(3) Å is, on the other hand, much longer than regular rhodium−carbon bonds. Recently, there was a report on formation of a C−C agostic metal (Ti) complex.[22] Although this type of interaction is still very rare, it is conceivable that the observed phenomena can be accounted for in terms of an agostic interaction. Notably, it was shown that in complex **11**, which is isostructural and isoelectronic to **9** but bearing a hydrogen atom instead of a methyl group in the ipso-position, the agostic character of the C_{ipso}−H bond is very prominent.[14]

Comparison and Interconversion of Methylene Arenium and σ-Arenium Complexes. The most pronounced difference between the reported methylene arenium complexes and the σ-arenium ones is in the amount of positive charge on the aromatic ring. The nature of the methylene arenium resonance hybrid is dependent on the relative contribution of the resonance aromatization−dearomatization forms. These resonance forms for methylene arenium complexes are most probably very different in energy (Scheme 3). The contribution of the benzylic form is not large,[23,24] the main contribution coming from the methylene arenium form, with positive charge on the ring. It is likely that the noncompensated, localized positive charge in M(III) benzylic species diminishes significantly the stability of the arene resonance form. In accordance with this is the tendency of increasing the arenium character upon an increase of the olefin complex stability in the order **15** < **2a** < **4**. Thus, lowering of the olefin complex stability leads to a larger relative contribution of the benzylic form.

Examining the spectroscopic and chemical properties of complexes **9a**,**b** reveals that the arenium character of these compounds is much less pronounced than in the case of methylene arenium complexes (vide supra). In this case the arenium−arene resonance hybrid is composed of two forms, closer in energy to each other

(19) Grove, D. M.; van Koten, G.; Ubbels, H. J. C. *Organometallics* **1982**, *1*, 1366.
(20) Lagunas, M.-C.; Gossage, R. A.; Spek, A. L.; van Koten, G. *Organometallics* **1998**, *17*, 731.
(21) Ortiz, J. V.; Havlas, Z.; Hoffmann, R. *Helv. Chim. Acta* **1984**, *67*, 1.
(22) Tomaszewski, R.; Hyla-Kryspin, I.; Mayne, C. L.; Arif, A. M.; Gleiter, R.; Ernst, R. *J. Am. Chem. Soc.* **1998**, *120*, 2959.
(23) For detailed NMR studies on organic carbocations see: Prakash, G. K. S.; Iyer, P. S. *Rev. Chem. Intermed.* **1988**, *9*, 65.
(24) For relevant references see: (a) Bollinger, J. M.; Comisarow, M. B.; Cupas, C. A.; Olah, G. A. *J. Am. Chem. Soc.* **1967**, *89*, 5687. (b) Olah, G. A.; Porter, R. D.; Jeuell, C. L.; White, A. M. *J. Am. Chem. Soc.* **1972**, *94*, 2044. (c) Olah, G. A.; Shamma, T.; Burrichter, A.; Rasul, G.; Prakash, G. K. S. *J. Am. Chem. Soc.* **1997**, *119*, 3407. (d) Van Pelt, P.; Buck, H. M. *Rec. Trav. Chim. Pays-Bas* **1973**, *92*, 1057.

(Scheme 3). The positive charge on the metal in the arene form can be compensated by an agostic interaction with the C−C bond, which is the case for the analogous compound with the C−H bond.[14] Thus, aromatization is a significant factor in the less positive charge on the ring of **9** as compared to methylene arenium complexes.

The arenium character, that is the positive charge on the ring, decreases in the order **4** > **2a** > **15** > **9** as evident from the NMR data. Interestingly, it is possible to convert **2a** into **15** and the latter into **9**, providing a route to convert one class of arenium complexes (methylene arenium) into another class (σ-arenium), resulting in the significant decrease of positive charge on the ring. Importantly, the aromatization−dearomatization balance can be controlled by the choice of metals and ancillary ligands. Moreover, it can be regulated by means of simple chemical transformations, as in the case of methylene arenium into σ-arenium transformation.

Conclusions

Stabilization of methylene arenium and σ-arenium compounds by transition metals, demonstrated in the present work, was achieved using different PCP ligands and two transition metals: rhodium and iridium. The protonation of metal aryl complexes to form stable methylene arenium complexes includes a mild conditions dearomatization process. The low-temperature study of this process revealed a major role of the metal center in the overall transformation including 1,2-methyl shift, β-hydride elimination, and hydride abstraction by deprotonation. The last step of the process is an unprecedented irreversible loss of triflic acid from a M(III) methylene arenium intermediate, which was characterized at low temperature.

Methylene arenium complexes represent a class of compounds in which most of the positive charge is located on the ring, rather than on the metal; that is, there is a minor contribution of the arene resonance form to the arene−arenium hybrid of the methylene arenium complexes. This is not the case for σ-arenium compounds, where the amount of positive charge on the ring is significantly smaller than in the methylene arenium complexes, as evident from the reactivity and spectroscopic data. There is more contribution of the arene resonance form in the σ-arenium complexes, probably due to its stabilization by an agostic interaction of the cationic metal center with the arene−alkyl C−C bond.

Aromatization−dearomatization interplay resulting in change of charge distribution can be decided by the choice of metals and ancillary ligands. Conversion of one class of compounds (methylene areniums) into another (σ-areniums) also provides a tool for regulating the amount of positive charge on the ring by means of simple chemical transformations.

Experimental Section

General Procedures. All operations with air- and moisture-sensitive compounds were performed in a nitrogen-filled glovebox (Vacuum Atmospheres with an MO-40 purifier). All solvents were reagent grade or better. Pentane, benzene, and THF were distilled over sodium/benzophenone ketyl. All solvents were degassed and stored under high-purity nitrogen after distillation. All deuterated solvents (Aldrich) were stored under high-purity nitrogen on molecular sieves (3 Å). Trifluoromethanesulfonic acid and trifluoromethanesulfonic acid-d_1 were purchased from Aldrich. 1-Bromo-2,4,6-trimethylbenzene was purchased from Aldrich and used as is.

^{1}H, ^{31}P, and ^{13}C NMR spectra were recorded at 400, 162, and 100 MHz, respectively, using a Bruker AMX400 spectrometer. ^{1}H and ^{13}C chemical shifts are reported in ppm downfield from TMS and referenced to the residual solvent. ^{31}P chemical shifts are in ppm downfield from H_3PO_4 and referenced to an external 85% phosphoric acid sample. All measurements were performed at 23 °C unless otherwise specified.

Complex 2a. To a solution of **1a**[9] (14 mg, 0.024 mmol) in 1 mL of dichloromethane was added 100 μL (≈1.2 equiv) of 0.3 M HOTf in dioxane at room temperature. Immediate color change from red to brown took place. After staying at room temperature for a few (5−10) minutes the color became dark green. The mixture was poured into 3 mL of pentane, and the resulting precipitate was filtered through a cotton pad, washed with pentane and benzene, and redissolved in dichloromethane. Evaporation of the solvent gave pure **2a** as a green solid in quantitative yield.

^{31}P{^{1}H} NMR (δ, ppm) (CD_2Cl_2): 17.55 (d, J_{RhP} = 98.0 Hz). ^{1}H NMR (δ, ppm): 8.60 (s, 1H, Ar−**H**), 4.84 (t, J_{PH} = 6.5 Hz, 2H, C=C**H**$_2$), 2.78 (AB quart. J_{HH} = 16.9 Hz, 4H, C**H**$_2$−P), 2.50 (s, 6H, Ar−C**H**$_3$), 1.51 (vt, J_{PH} = 7.2 Hz, 18H, t-Bu), 1.32 (vt, J_{PH} = 7.0 Hz, 18 H, t-Bu). ^{13}C{^{1}H} NMR (δ, ppm): 160.80 (s, **Ar**), 151.23 (s, **Ar**), 139.34 (t, J_{PC} = 4.6 Hz, **Ar**), 93.37 (dt, J_{RhC} = 8.3 Hz, J_{PC} = 3.1 Hz, **C**=CH$_2$), 41.47 (br dt, J_{RhC} = 24.7 Hz, J_{PC} = 2.7 Hz, C=**C**H$_2$), 38.13 (td, J_{PC} = 6.9 Hz, J_{RhC} = 1.1 Hz, **C**(CH$_3$)$_3$), 37.90 (t, J_{PC} = 6.6 Hz, **C**(CH$_3$)$_3$), 31.09 (t, J_{PC} = 2.4 Hz, C(**C**H$_3$)$_3$), 29.72 (t, J_{PC} = 1.8 Hz, C(**C**H$_3$)$_3$), 23.38 (t, J_{PC} = 8.0 Hz, **C**H$_2$−P), 19.83 (s, Ar−**C**H$_3$).

Elemental Anal. Found (Calcd): C 46.55 (46.77), H 6.96 (6.83).

Complex 1c. The new ligand MeO$_2$C−DTBPM was synthesized in 18% overall yield in several steps starting from 1-Br-2,4,6-trimethyl benzene (Scheme 1).

^{31}P{^{1}H} NMR ($CDCl_3$): 27.43 (s). ^{1}H NMR: 3.84 (s, 3H, CO$_2$C**H**$_3$), 2.90 (d, J_{PH} = 2.13 Hz, 4H, Ar−C**H**$_2$−P), 2.63 (s, 3H, 2 Ar−C**H**$_3$), 2.32 (s, 6H, Ar−C**H**$_3$), 1.09 (d, J_{PH} = 10.6 Hz, 36H, (C**H**$_3$)$_3$C−P). ^{13}C{^{1}H} NMR: 172.14 (s, **C**O$_2$Me), 136.65 (br s, **Ar**), 136.38 (d, J_{PC} = 6.9 Hz, **Ar**), 134.52 (**Ar**), 129.13 (s, **Ar**), 51.78 (s, CO$_2$**C**H$_3$), 32.34 (d, J_{PC} = 24.6 Hz, (CH$_3$)$_3$**C**−P), 29.83 (d, J_{PC} = 13.0 Hz, (**C**H$_3$)$_3$C−P), 24.06 (d, J_{PC} = 28.7 Hz, Ar−**C**H$_2$−P), 20.32 (t, J_{PC} = 10.7 Hz, Ar−**C**H$_3$), 18.88 (d, J_{PC} = 7.1 Hz, 2 × **C**H$_3$−Ar). IR (film): 1730 cm^{-1} (s).

To a benzene solution (2 mL) of MeO$_2$C−DTBPM (28 mg, 0.056 mmol) was added 2 mL of a benzene solution of [Rh(COE)$_2$Cl]$_2$ (20 mg, 0.028 mmol). The mixture was stirred at room temperature for 18 h, resulting in color change to dark red. Evaporation of the solvent resulted in formation of **1c** as a red solid in quantitative yield.

^{31}P{^{1}H} NMR (C_6D_6): 55.97 (d, J_{RhP} = 117.9 Hz). ^{1}H NMR: 3.63 (s, 3H, CO$_2$C**H**$_3$), 2.94 (AB quartet, J_{HH} = 17.5 Hz, 4H, Ar−C**H**$_2$−P), 2.27 (s, 6H, 2 Ar−C**H**$_3$), 1.65 (td, J_{PH} = 5.0 Hz, J_{RhH} = 2.9 Hz, Rh−C**H**$_3$), 1.34 (t, J_{PH} = 6.5 Hz, 18H, 2 (C**H**$_3$)$_3$C−P), 1.15 (t, J_{PH} = 6.1 Hz, 18H, 2 (C**H**$_3$)$_3$C−P). ^{13}C{^{1}H} NMR: 171.85 (t, J_{PH} = 1.0 Hz, **C**O$_2$Me), 171.35 (dt, J_{RhC} = 34.5 Hz, J_{PC} = 2.0 Hz, C$_{ipso}$, Rh−**Ar**), 146.92 (td, J_{PC} = 9.1 Hz, J_{RhC} = 0.9 Hz, Rh−**Ar**), 127.36 (td, J_{PC} = 7.9 Hz, J_{RhC} = 1.5 Hz, Rh−**Ar**), 36.32 (td, J_{PC} = 7.2 Hz, J_{RhC} = 1.5 Hz, (CH$_3$)$_3$**C**−P), 36.10 (t, J_{PC} = 7.6 Hz, (CH$_3$)$_3$**C**−P), 31.02 (t, J_{PC} = 2.4 Hz, (**C**H$_3$)$_3$C−P), 30.64 (td, J_{PC} = 9.3 Hz, J_{RhC} = 2.7 Hz, Ar−**C**H$_2$−P), 29.51 (t, J_{PC} = 2.0 Hz, (**C**H$_3$)$_3$C−P), 19.80 (s, **C**H$_3$−Ar), 2.15 (dt, J_{RhC} = 30.5 Hz, J_{PC} = 5.8 Hz, Rh−**C**H$_3$). IR (film): 1725 cm^{-1} (s).

Elemental Anal. Found (Calcd): C 55.07 (55.02), H 8.10 (8.28).

Complex 2c. Complex **2c** was prepared analogously to **2a**.

$^{31}P\{^1H\}$ NMR (δ, ppm) (CD_2Cl_2): 16.65 (d, J_{RhP} = 97.3 Hz). ^1H NMR (δ, ppm): 4.94 (t, J_{PH} = 6.6 Hz, 2H, C=C**H**$_2$), 3.98 (s, 3H, CO_2C**H**$_3$), 2.84 (AB quart. J_{HH} = 16.9 Hz, 4H, C**H**$_2$−P), 2.49 (s, 6H, Ar−C**H**$_3$), 1.56 (vt, J_{PH} = 7.2 Hz, 18H, t-Bu), 1.39 (vt, J_{PH} = 7.0 Hz, 18 H, t-Bu). $^{13}C\{^1H\}$ NMR (δ, ppm): 179.01 (s, **C**O_2Me), 159.77 (s, **Ar**), 150.16 (br s, **Ar**), 135.45 (t, J_{PC} = 4.6 Hz, **Ar**), 95.48 (dt, J_{RhC} = 8.1 Hz, J_{PC} = 3.3 Hz, **C**=CH_2), 39.59 (dt, J_{RhC} = 24.6 Hz, J_{PC} = 3.1 Hz, C=**C**H_2), 37.98 (td, J_{PC} = 6.9 Hz, J_{RhC} = 1.2 Hz, **C**$(CH_3)_3$), 37.81 (t, J_{PC} = 6.6 Hz, **C**$(CH_3)_3$), 30.86 (t, J_{PC} = 2.4 Hz, C(**C**$H_3)_3$), 29.35 (t, J_{PC} = 1.7 Hz, C(**C**$H_3)_3$), 23.24 (t, J_{PC} = 8.0 Hz, **C**H_2−P), 16.98 (s, Ar−**C**H_3). IR (film): 1733 cm^{-1} (s).

Complex 4. To a solution of **3**[9] (10 mg, 0.015 mmol) in 1 mL of dichloromethane was added 60 μL (≈1.2 equiv) of HOTf at −78 °C. The mixture was gradually warmed to ambient temperature during 30 min. A color change from red to green took place, and $^{31}P\{^1H\}$ NMR revealed quantitative formation of **4**. Workup similar to that of the rhodium analogue gave pure **4** as a green solid in an almost quantitative yield.

$^{31}P\{^1H\}$ NMR ($CDCl_3$): 12.70 (s). ^1H NMR: 9.20 (s, 1H, **Ar**), 5.18 (t, J_{PH} = 6.6 Hz, 2H, C=C**H**$_2$), 2.91 (dvt, the left part of an AB pattern, J_{HH} = 17.1 Hz, J_{PH} = 4.9 Hz, 2H, Ar−C**H**$_2$P), 2.50 (vt, the signal belongs to the right part of an AB pattern, J_{PH} = 3.5 Hz, 1H, Ar−C**H**$_2$P), 2.26 (br s, 8H, 2 C**H**$_3$−Ar overlapped with the signal of Ar−C**H**$_2$P belonging to the right part of an AB pattern), 1.47 (vt, J_{PH} = 7.1 Hz, 18H, 2 (C**H**$_3)_3$-CP), 1.32 (vt, J_{PH} = 6.8 Hz, 18H, 2(C**H**$_3)_3$CP). $^{13}C\{^1H\}$ NMR: 169.28 (s, **Ar**), 152.59 (s, **Ar**), 138.74 (t, J_{PC} = 4.5 Hz, **Ar**), 83.14 (br s, **C**=CH_2), 37.61 (vt, J_{PC} = 8.9 Hz, $(CH_3)_3$**C**P), 37.17 (vt, J_{PC} = 9.9 Hz, $(CH_3)_3$**C**P), 35.48 (br s, C=**C**H_2), 31.06 (vt, J_{PC} = 1.8 Hz, (**C**$H_3)_3$CP), 29.53 (br s, (**C**$H_3)_3$CP), 24.56 (vt, J_{PC} = 11.6 Hz, Ar−**C**H_2P), 19.21 (d, J_{PC} = 1.9 Hz, **C**H_3−Ar).

Complex 5 was the only species observed upon protonation of **1a** by 5 equiv of HOTf in $CDCl_3$ at −50 °C. $^{31}P\{^1H\}$ NMR (δ, ppm) ($CDCl_3$): 52.52 (d, J_{RhP} = 92.7 Hz). ^1H NMR (δ, ppm): −21.38 (dt, J_{RhH} = 34.2 Hz, J_{PH} = 12.3 Hz, 1H, Rh−**H**), 3.47 (br s, 2H, C=C**H**$_2$), 3.04 (AB quart. J_{HH} = 15.6 Hz, 4H, C**H**$_2$−P), 2.00 (s, 6H, Ar−C**H**$_3$), 1.42 (br m, 36H, t-Bu). $^{13}C\{^1H\}$ NMR (δ, ppm): 160.41 (s, **Ar**), 150.83 (br s, **Ar**), 142.49 (t, J_{PC} = 5.2 Hz, **Ar**), 120.24 (m, overlapped with **C**F_3SO_3, **C**=CH_2), 48.25 (br d, J_{RhC} = 7.4 Hz, C=**C**H_2), 38.07 (t, J_{PC} = 7.8 Hz, **C**$(CH_3)_3$), 36.77 (td, J_{PC} = 7.0 Hz, J_{RhC} = 0.8 Hz, **C**$(CH_3)_3$), 30.74 (br s, C(**C**$H_3)_3$), 28.87 (br s, C(**C**$H_3)_3$), 20.76 (s, Ar−**C**H_3), 18.08 (t, J_{PC} = 8.0 Hz, **C**H_2−P).

Protonation of Complex 3 at Low Temperature. A $CDCl_3$ solution of triflic acid (9 equiv) was added to a $CDCl_3$ solution of **3** at −78 °C. In the $^{31}P\{^1H\}$ NMR of the mixture, kept at −55 °C for 15 min, four main signals, all singlets, were observed: at 49.03, 44.61 (starting complex **3**), 43.38, and 39.21 ppm, in a ratio of 10:4:5:15, respectively. Keeping the mixture at −55 °C for 40 min resulted in almost complete disappearance of the product at 43.38 ppm. At this point formation of the final product **4** (see Scheme 1) started. After 15 min at −40 °C $^{31}P\{^1H\}$ NMR revealed formation of two main products (singlets at 49.11 and 39.47 ppm, ratio 1:2, respectively). The signals attributed to product at 49.11 ppm, complex **6**, in ^1H NMR (ppm): 3.44 (br s, 1H, **H**−ipso-C, no signal when DOTf was used), 3.05 (unresolved AB pattern, 4H, Ar−C**H**$_2$−P), 2.24 (s, 6H, C**H**$_3$−Ar), 1.84 (t, J = 4,9 Hz, 3H, C**H**$_3$−Ir). The signals attributed to product at 39.47 ppm, complex **7**, in ^1H NMR (ppm): 3.73 (unresolved triplet, 2H, =CH2), 3.33 (dvt, the left part of an AB pattern, J_{HH} = 16.2 Hz, J_{HP} = 3.7 Hz, 2H, Ar−C**H**$_2$−P), 2.82 (bd, the right part of an AB pattern with unresolved PH coupling Ar−C**H**$_2$−P), 1.96 (s, 6H, C**H**$_3$−Ar), −35.78 (t, J_{HP} = 8.7 Hz, **H**−Ir). The signal assignment is done on the grounds of integration and obseration of **7** as the main product at 0 °C.

As the temperature was gradually raised to 0 °C, complex **7** became the main product in the reaction mixture (∼70%, observed by $^{31}P\{^1H\}$ NMR). The hydride signal integration did not change when DOTf was used. Only a small amount of the final product, complex **4**, was observed. As the temperature was raised to 20 °C, slow formation of the final product **4** took place. Keeping the reaction mixture at room temperature overnight resulted in formation of **4** (90%) and decomposition products.

Complex 7 (0 °C): $^{31}P\{^1H\}$ NMR (δ, ppm): 39.47; ^1H NMR (δ, ppm): 3.75 (t, J_{PH} = 3.4 Hz, 2H, =C**H**$_2$), 3.33 (dvt, the left part of an AB pattern, J_{HH} = 16.2 Hz, 2H, Ar−C**H**$_2$−P), 2.82 (br d, the right part of an AB pattern, 2H, Ar−C**H**$_2$−P), 1.96 (s, 6H, C**H**$_3$−Ar), 1.43 (apparent quartet, J_{PH} = 7.2 Hz, 36H, C(C**H**$_3)_3$), −35.78 (t, J_{PH} = 8.7 Hz, 1H, **H**−Ir). The signal assignment was confirmed by $^1H\{^{31}P\}$ NMR.

Complex 9a. To a solution of **1a**[9] (16 mg, 0.028 mmol) in 1 mL of THF was added 8 mg (0.031 mmol) of AgOTf in 1 mL of THF at room temperature. Upon staying for 30 min in the dark, AgCl precipitated. The precipitate was filtered off, and carbon monoxide was passed through the clean yellow solution for a few seconds. The ^{31}P NMR spectrum showed quantitative formation of **9a**. The solvent was evaporated, and the resulting yellow solid was washed with pentane and dried in a vacuum to give 18 mg of **9a** (89%).

$^{31}P\{^1H\}$ NMR (δ, ppm) ($CDCl_3$): 25.14 (d, J_{RhC} = 99.1 Hz). ^1H NMR (δ, ppm): 7.19 (s, Ar−**H**), 3.50 (t, J_{PH} = 4.2 Hz, 4H, C**H**$_2$−P), 2.59 (s, 3H, ipso-C**H**$_3$), 2.40 (t, J_{PH} = 1.64 Hz, 6H, Ar(C**H**$_3)_2$), 1.44 (vt, J_{PH} = 7.3 Hz, 18H, t-Bu), 1.24 (vt, J_{PH} = 7.3 Hz, 18 H, t-Bu). $^{13}C\{^1H\}$ NMR (δ, ppm): 189.21 (dt, J_{RhC} = 97.1 Hz, J_{PC} = 12.4 Hz, Rh−**C**O), 143.10 (d, J_{PC} = 1.0 Hz, **Ar**), 139.71 (br td, J_{PC} = 3.9 Hz, J_{RhC} = 1.4 Hz, **Ar**), 134.93 (td, J_{PC} = 5.1 Hz, J_{RhC} = 1.1 Hz, **Ar**), 108.53 (td, J_{PC} = 4.2 Hz, J_{RhC} = 2.3 Hz, ipso-**C**), 37.87 (td, J_{PC} = 8.8 Hz, J_{RhC} = 1.3 Hz, **C**$(CH_3)_3$), 36.54 (td, J_{PC} = 7.9 Hz, J_{RhC} = 1.0 Hz, **C**$(CH_3)_3$), 30.63 (t, J_{PC} = 2.1 Hz, C(**C**$H_3)_3$), 29.72 (t, J_{PC} = 2.5 Hz, C(**C**$H_3)_3$), 23.08 (td, J_{PC} = 8.8 Hz, J_{RhC} = 1.8 Hz, **C**H_2−P), 20.44 (s, Ar(**C**$H_3)_2$), 8.23 (br m, ipso-**C**H_3). IR (film): 1969 cm^{-1} (s).

Elemental Anal. Found (Calcd): C 48.30 (48.60), H 6.98 (7.03).

Complex 9b. Complex **9b** was prepared analogously to **9a** from $(PhCH_2)RhCl[C_6H(CH_3)_2(CH_2P(t\text{-}Bu)_2)_2]$[25] in 80% yield. $^{31}P\{^1H\}$ NMR (δ, ppm) ($CDCl_3$): 22.00 (d, J_{RhC} = 101.2 Hz). ^1H NMR (δ, ppm): 7.50 (s, 1H, Ar−**H**), 7.15 (m, 3H), 6.23 (m, 2H), 4.95 (s, 2H, ipso-C**H**$_2$Ph), 3.52 (AB quart., J_{HH} = 19.9 Hz, 4H, C**H**$_2$−P), 2.49 (s, 6H, Ar(C**H**$_3)_2$), 1.49 (vt, J_{PH} = 7.3 Hz, 18H, t-Bu), 1.29 (vt, J_{PH} = 7.2 Hz, 18 H, t-Bu). $^{13}C\{^1H\}$ NMR (δ, ppm): 187.11 (dt, J_{RhC} = 93.1 Hz, J_{PC} = 12.4 Hz, Rh−**C**O), 146.92 (m, **Ar**), 142.87 (br m, **Ar**), 138.55 (d, J_{RhC} = 2.0 Hz, **Ar**), 136.07 (td, J_{PC} = 5.1 Hz, J_{RhC} = 1.8 Hz, **Ar**), 129.30 (s, **Ar**), 127.60 (s, **Ar**), 126.28 (s, **Ar**), 112.35 (br m, ipso-**C**), 37.65 (td, J_{PC} = 8.1 Hz, J_{RhC} = 1.2 Hz, **C**$(CH_3)_3$), 35.77 (td, J_{PC} = 7.9 Hz, J_{RhC} = 0.9 Hz, **C**$(CH_3)_3$), 29.98 (t, J_{PC} = 2.4 Hz, C(**C**$H_3)_3$), 29.57 (t, J_{PC} = 2.5 Hz, C(**C**$H_3)_3$), 27.57 (br s, ipso-**C**H_2Ph), 23.29 (br t, J_{PC} = 8.2 Hz, **C**H_2−P), 20.13 (s, Ar(**C**$H_3)_2$). IR (film): 1967 cm^{-1} (s).

Complex 12. To a solution of **2a** in CH_2Cl_2 (20 mg, 0.028 mmol) was added NEt_3 (5 μL, 0.050 mmol). Immediate color change from green to red took place, and formation of the single product **12** was detected by $^{31}P\{^1H\}$ NMR. The solvent was evaporated, and the resulting red solid was washed with pentane and redissolved in benzene. Filtration through a cotton pad followed by evaporation of the solvent resulted in pure **12** (15 mg, 94%).

$^{31}P\{^1H\}$ NMR (δ, ppm) (C_6D_6): 51.18 (J_{PaPb} = 376.3 Hz, J_{RhPa} = 124.7 Hz, J_{RhPb} = 118.0 Hz). ^1H NMR (δ, ppm): 5.73 (s, 1H, Ar−**H**), 5.28 (d, J_{PH} = 3.4 Hz, 1H, C=C**H**−P), 3.01 (AB quart., 2H, Rh−(C=C**H**$_2$)), 2.16 (AB quart. J_{HH} = 16.7 Hz, 2H, C**H**$_2$−P), 1.78 (s, 3H, Ar−C**H**$_3$), 1.54 (br t, 3H, Ar−C**H**$_3$), 1.46 (d, J_{PH} = 12.5 Hz, 9H, t-Bu), 1.41 (d, J_{PH} = 12.1 Hz, 9H, t-Bu), 1.40 (d, J_{PH} = 11.7 Hz, 9H, t-Bu), 1.28 (d, J_{PH} = 12.2 Hz, 9H, t-Bu). $^{13}C\{^1H\}$ NMR (δ, ppm): 170.70 (d, J_{PC} = 15.6 Hz, **Ar**), 143.90 (dt, J_{RhC} = 4.5 Hz, J_{PC} = 0.9 Hz, **Ar**), 133.36 (d, J_{PC} =

(25) Milstein, D. Unpublished results.

1.9 Hz, **Ar**), 123.31 (s, **Ar**), 120.75 (d, J_{PC} = 12.6 Hz, **Ar**), 102.97 (d, J_{PC} = 31.7 Hz, C=**C**H−P), 75.30 (ddd, J_{RhC} = 15.3 Hz, J_{PaC} = 5.0 Hz, J_{PbC} = 5.1 Hz, Rh−(**C**=CH_2)), 57.73 (dt, J_{RhC} = 18.1 Hz, J_{PC} = 3.9 Hz, Rh−(C=**C**H_2)), 30.90 (m, 2 C(**C**H_3)$_3$), 30.23 (dd, J_{PaC} = 2.8 Hz, J_{PbC} = 0.8 Hz, C(**C**H_3)$_3$), 29.41 (dd, J_{PC} = 4.5 Hz, J_{PaC} = 1.2 Hz, C(**C**H_3)$_3$), 21.54 (d, J_{PC} = 16.7 Hz, **C**H_2−P), 19.66 (s, Ar−**C**H_3), 19.56 (d, J_{PC} = 1.6 Hz, Ar−**C**H_3).

Complex 13. NEt_3 (5 mg, 0.052 mmol) was added to 3 mL of a CH_2Cl_2 solution of complex **4** (10 mg, 0.012 mmol). Immediate color change from green-brown to red took place. The $^{31}P\{^1H\}$ NMR spectrum of the reaction mixture revealed formation of the xylylene complex **13** in 90% yield. Cleaner reaction was observed when complex **4** was passed through a small (Pasteur pipet) Alumina III column, using THF as an eluent. A red fraction was collected and evaporation of the solvent resulted in the product **13** as a red solid in nearly quantitative yield. Upon addition of HOTf to a $CDCl_3$ solution of complex **13**, a color change from red to green-brown was observed. $^{31}P\{^1H\}$ and ^1H NMR revealed quantitative formation of the methylene arenium complex **4**.

The xylylene ring is depicted as Ar − $^{31}P\{^1H\}$ NMR ($CDCl_3$) 38.75 (d, the left part of an AB pattern, $^2J_{PP}$ = 360.1 Hz, 1P), 35.12 (d, the right part of an AB pattern, 1P). ^1H NMR ($CDCl_3$): 5.87 (s, 1H, Ir−**Ar**), 5.40 (vt, J_{PH} = 3.6 Hz, 1H, P=C**H**−Ar), 2.66 (dd, J_{PH} = 7.2 Hz, J_{PH} = 2.2 Hz, 1H, C=C$\mathbf{H}_2$), 2.52 (dd, the left part of an AB pattern, J_{HH} = 16.9 Hz, J_{PH} = 9.7 Hz, 1H, Ar−C$\mathbf{H}_2$P), 2.36 (br. dd, the right part of an AB pattern, J_{PH} = 7.5 Hz, 1H, Ar−C$\mathbf{H}_2$P), 2.20 (dd, J_{PH} = 8.0 Hz, J_{PH} = 2.8 Hz, 1H, C=C$\mathbf{H}_2$), 1.91 (bs, 3H, C$\mathbf{H_3}$−Ar), 1.69 (bs, 3H, C$\mathbf{H_3}$−Ar), 1.38 (m, 36H, 4 (C$\mathbf{H}_3$)$_3$C−P) Assignment of ^1H NMR signals was confirmed by $^1H\{^{31}P\}$ NMR and 2D $^{13}C-^1H$ correlation.

$^{13}C\{^1H\}$ NMR ($CDCl_3$): 172.15 (dd, J_{PC} = 13.6 Hz, J_{PC} = 2.9 Hz **Ar**−Ir), 144.80 (dd, J_{PC} = 4.0 Hz, J_{PC} = 1.8 Hz, **Ar**−Ir), 133.32 (s, C_{para}, **Ar**−Ir), 125.94 (dd, J_{PC} = 14.9 Hz, J_{PC} = 3.0 Hz, **Ar**−Ir), 119.15 (dd, J_{PC} = 11.8 Hz, J_{PC} = 1.9 Hz, **Ar**−Ir), 102.62 (dd, J_{PC} = 37.6 Hz, J_{PC} = 3.0 Hz, P=**C**H−Ar), 57.73 (dd, J_{PC} = 5.6 Hz, J_{PC} = 3.7 Hz, **C**=CH_2), 42.26 (vt, $J_{PC,virt}$ = 3.3 Hz, C=**C**H_2), 36.72 (m, overlapped 2 $(CH_3)_3$**C**−P), 35.63 (dd, J_{PC} = 10.1 Hz, J_{PC} = 5.7 Hz, $(CH_3)_3$**C**−P), 35.20 (dd, J_{PC} = 13.2 Hz, J_{PC} = 6.2 Hz, $(CH_3)_3$**C**−P), 30.86 (dd, J_{PC} = 3.7 Hz, J_{PC} = 1.7 Hz, (**C**H_3)$_3$C−P), 30.70 (dd, J_{PC} = 2.9 Hz, J_{PC} = 1.1 Hz, (**C**H_3)$_3$C−P), 30.01 (dd, J_{PC} = 2.7 Hz, J_{PC} = 1.1 Hz, (**C**H_3)$_3$C−P), 29.40 (dd, J_{PC} = 3.7 Hz, J_{PC} = 1.5 Hz, (**C**H_3)$_3$C−P), 21.45 (d, J_{PC} = 21.8 Hz, Ar−**C**H_2−P), 19.92 (s, **C**H_3−Ar), 19.83 (s, **C**H_3−Ar). Assignment of $^{13}C\{^1H\}$ NMR signals was confirmed by ^{13}C DEPT 135 and 2D $^{13}C-^1H$ correlation.

Elemental Anal. Found (Calcd): C 48.61 (48.96), H 7.15 (7.31).

Complex 14. When carbon monoxide was bubbled through a solution of **2a** in CD_2Cl_2, immediate color change from green to red took place and quantitative formation of the pentacoordinate CO adduct **14** was observed. The reaction appeared to be reversible, with complex **2a** being recovered upon moderate heating of a methylene chloride solution of **14** or upon drying of **14** in a vacuum.

$^{31}P\{^1H\}$ NMR (δ, ppm) (CD_2Cl_2): 38.46 (d, J_{RhP} = 75.7 Hz). ^1H NMR (δ, ppm): 7.75 (s, 1H, Ar−**H**), 4.15 (t, J_{PH} = 6.3 Hz, 2H, C=C$\mathbf{H}_2$), 3.33 (AB quart. J_{HH} = 16.4 Hz, 4H, C$\mathbf{H}_2$−P), 2.44 (s, 6H, Ar−C$\mathbf{H}_3$), 1.51 (m, 32H, t-Bu). $^{13}C\{^1H\}$ NMR (δ, ppm): 188.27 (d, J_{RhC} = 88.8 Hz, Rh−**C**O), 146.77 (s, **Ar**), 145.27 (t, J_{PC} = 2.7 Hz, **Ar**), 137.92 (t, J_{PC} = 5.4 Hz, **Ar**), 107.69 (td, J_{PC} = 6.8 Hz, J_{RhC} = 3.4 Hz, **C**=CH_2), 42.03 (t, J_{PC} = 7.2 Hz, **C**$(CH_3)_3$), 39.18 (td, J_{PC} = 5.5 Hz, J_{RhC} = 1.5 Hz, **C**$(CH_3)_3$), 39.10 (dt, J_{RhC} = 15.0 Hz, J_{PC} = 2.5 Hz, C=**C**H_2), 29.94 (t, J_{PC} = 1.5 Hz, C(**C**H_3)$_3$), 22.29 (t, J_{PC} = 9.9 Hz, **C**H_2−P), 19.99 (s, Ar−**C**H_3).

Complex 15. To a solution of **2a** (20 mg, 0.028 mmol) in CH_2Cl_2 (0.6 mL) was bubbled carbon monoxide for 1 min, resulting in clean formation of **14**, as was detected by $^{31}P\{^1H\}$ NMR spectroscopy. To this solution ca. 15 equiv of Me_3SiOTf (75 μL, 0.416 mmol) was added. The mixture was allowed to stay for 12 h, and the solution was poured into 3 mL of pentane. The orange precipitate was filtered through a cotton pad, washed thoroughly with pentane, and redissolved in CH_2Cl_2. Evaporation of the solvent resulted in **15** as an orange solid (yield 19 mg, the product was contaminated with small amount of **2a**, ca. 5%).

$^{31}P\{^1H\}$ NMR (δ, ppm) ($CDCl_3$): 35.65 (d, J_{RhP} = 76.3 Hz). ^1H NMR (δ, ppm): 7.98 (s, 1H, Ar−**H**), 4.47 (t, J_{PH} = 6.1 Hz, 2H, C=C$\mathbf{H}_2$), 3.53 (AB quart. J_{HH} = 17.0 Hz, 4H, C$\mathbf{H}_2$−P), 2.53 (s, 6H, Ar−C$\mathbf{H}_3$), 1.54 (vt, J_{PH} = 7.7 Hz, 18H, t-Bu), 1.36 (vt, J_{PH} = 7.7 Hz, 18 H, t-Bu). $^{13}C\{^1H\}$ NMR (δ, ppm): 185.50 (d, J_{RhC} = 93.9 Hz, Rh−**C**O), 150.42 (s, **Ar**), 149.69 (s, **Ar**), 139.19 (t, J_{PC} = 4.5 Hz, **Ar**), 105.61 (br s, **C**=CH_2), 42.32 (br d, C=**C**H_2), 41.76 (t, J_{PC} = 6.6 Hz, **C**$(CH_3)_3$), 39.25 (td, J_{PC} = 5.7 Hz, J_{RhC} = 1.4 Hz, **C**$(CH_3)_3$), 30.65 (s, C(**C**H_3)$_3$), 29.18 (s, C(**C**H_3)$_3$), 22.36 (t, J_{PC} = 10.3 Hz, **C**H_2−P), 20.14 (s, Ar−**C**H_3). IR (film): 2063 cm^{-1}.

Complex 16. Complex **16** was prepared by reacting **9a** (15 mg, 0.021 mmol) with 1.1 equiv of NEt_3 (4 μL, 0.029 mmol) in THF (1 mL). The yellow solution was immediately formed. The solvent was evaporated, and the resulting yellow solid was extracted with pentane and filtered through a cotton pad. Evaporation of pentane gave pure **16** (11 mg, 0.019 mmol). Yield: 93%.

$^{31}P\{^1H\}$ NMR (δ, ppm) (C_6D_6): 109.73 (d, J_{RhC} = 170.5 Hz). ^1H NMR (δ, ppm): 6.41 (s, Ar−**H**), 3.40 (AB quart., J_{HH} = 14.3 Hz, 4H, C$\mathbf{H}_2$−P), 2.34 (td, J_{PH} = 10.9 Hz, J_{RhH} = 2.2 Hz, 2H, Rh−C$\mathbf{H}_2$), 2.29 (s, 6H, Ar(C$\mathbf{H}_3$)$_2$), 1.36 (vt, J_{PH} = 6.1 Hz, 18H, t-Bu), 1.10 (vt, J_{PH} = 5.9 Hz, 18 H, t-Bu). $^{13}C\{^1H\}$ NMR (δ, ppm): 201.17 (dt, J_{RhC} = 64.9 Hz, J_{PC} = 13.5 Hz, Rh−**C**O), 143.12 (td, J_{PC} = 3.7 Hz, J_{RhC} = 1.0 Hz, **Ar**), 130.53 (t, J_{PC} = 2.8 Hz, **Ar**), 127.67 (br s, **Ar**), 121.76 (s, **Ar**), 37.75 (br m, **C**$(CH_3)_3$), 36.24 (td, J_{PC} = 6.3 Hz, J_{RhC} = 1.5 Hz, **C**$(CH_3)_3$), 30.65 (t, J_{PC} = 2.4 Hz, C(**C**H_3)$_3$), 30.34 (t, J_{PC} = 3.5 Hz, C(**C**H_3)$_3$), 22.81 (t, J_{PC} = 7.0 Hz, **C**H_2−P), 22.13 (dt, J_{RhC} = 12.4 Hz, J_{PC} = 5.2 Hz, Rh−**C**H_2), 20.17 (s, Ar(**C**H_3)$_2$). IR (film): 1906 cm^{-1} (s).

Crystal Structure Determination. X-ray Analysis of the Structure of 2a. Complex **2a** was crystallized from CH_2Cl_2/THF (1:1) mixture at room temperature to give green crystals.

Crystal data: $C_{28}H_{49}ClF_3O_3P_2RhS$, green needle, 0.1 × 0.1 × 0.05 mm^3, triclinic, $P\bar{1}$, a = 8.733(2) Å, b = 13.970(3) Å, c = 14.469(3) Å, α = 71.95(3)°, β = 78.75(3)°, γ = 84.65(3)° from 25 reflections, T = 110 K, V = 1645.1(6) $Å^3$, Z = 2, F_w = 723.03, D_c = 1.460 Mg/m^3, μ = 0.805 mm^{-1}.

Data collection and treatment: Rigaku AFC5R four-circle diffractometer, Mo Kα, graphite monochromator (λ = 0.710 73 Å), 7962 reflections collected, 2.38° ≤ θ ≤ 27.55°, −10 ≤ h ≤ 11, −18 ≤ k ≤ 17, −18 ≤ l ≤ 3, ω scan method, scan width = 1.2°, scan speed 2°/min, typical half-height peak width = 0.45°, 3 standards were collected 47 times each, with a 5% change in intensity, 7520 independent reflections (R_{int} = 0.0740).

Solution and Refinement. The structure was solved by Patterson methods (SHELXS-93). Full-matrix least-squares refinement was based on F^2 (SHELXL-93). Idealized hydrogens were placed and refined in a riding mode, with the exception of H10A and H10B on C10, which were located in the difference map and refined independently: 374 parameters with no restraints, final R_1 = 0.0773 (based on F^2) for data with $I > 2\sigma I$ and, R_1 = 0.0987 for all data based on 7520 reflections, goodness-of-fit on F^2 = 1.051, largest electron density = 1.938 e/$Å^{-3}$.

X-ray Analysis of the Structure of 9c. Complex **9c** was crystallized from a THF/CH_2Cl_2 mixture at room temperature.

Crystal data: $C_{30}H_{54}BF_4OP_2Rh$, orange-red prisms, 0.2 × 0.2 × 0.2 mm^3, triclinic, $P\bar{1}$, a = 12.497(3) Å, b = 15.705(5) Å, c = 8.622(3) Å, α = 105.51°, β = 93.35°, γ = 99.15°, from 25

reflections, $T = 110$ K, $V = 1600.7(8)$ Å^3, $Z = 2$, $F_w = 682.39$, $D_c = 1.416$ Mg/m^3, $\mu = 0.679$ mm^{-1}.

Data collection and treatment: Rigaku AFC5R four-circle diffractometer, Mo Kα, graphite monochromator ($\lambda = 0.710\ 73$ Å), 7977 reflections collected, $2.75° \leq \theta \leq 27.66°$, $-16 \leq h \leq 16$, $-19 \leq k \leq 20$, $-11 \leq l \leq 3$, ω scan method, scan width = 1.2°, scan speed 4°/min, typical half-height peak width = 0.45°, 3 standards were collected 90 times each, with a 4% change in intensity, 7353 independent reflections ($R_{int} = 0.0251$).

Solution and Refinement. The structure was solved by direct methods (SHELXS-96). Full-matrix least-squares refinement was based on F^2 (SHELXL-96). Idealized hydrogens were placed and refined in a riding mode. 381 parameters with 1 restraint, final $R_1 = 0.0358$ (based on F^2) for data with $I > 2\sigma I$ and, $R_1 = 0.0402$ for all data based on 7353 reflections, goodness-of-fit on $F^2 = 1.087$, largest electron density = 1.003 e/Å^{-3}.

The data were not corrected for absorption.

Acknowledgment. This work was supported by the Israel Science Foundation, Jerusalem, Israel, and by the MINERVA Foundation, Munich, Germany. D.M. is the holder of the Israel Matz professorial chair of organic chemistry.

Supporting Information Available: Tables of crystal data and structure refinement, atomic coordinates, bond lengths and angles, anisotropic displacement parameters, and hydrogen atom coordinates for complexes **2a**, and **9c**. This material is available free of charge via the Internet at http://pubs.acs.org.

OM980960I